# Thermodynamic and Kinetic Framework of Selenocysteyl-tRNA^Sec Recognition by Elongation Factor SelB*

**Alena Paleskava, Andrey L. Konevega, and Marina V. Rodnina**[1]

*From the Department of Physical Biochemistry, Max-Planck-Institute for Biophysical Chemistry, Am Fassberg 11, 37077 Göttingen, Germany*

**SelB is a specialized translation elongation factor that delivers selenocysteyl-tRNA^Sec (Sec-tRNA^Sec) to the ribosome. Here we show that Sec-tRNA^Sec binds to SelB·GTP with an extraordinary high affinity ($K_d$ = 0.2 pM). The tight binding is driven enthalpically and involves the net formation of four ion pairs, three of which may involve the Sec residue. The dissociation of tRNA from the ternary complex SelB·GTP·Sec-tRNA^Sec is very slow ($0.3\ h^{-1}$), and GTP hydrolysis accelerates the release of Sec-tRNA^Sec by more than a million-fold (to $240\ s^{-1}$). The affinities of Sec-tRNA^Sec to SelB in the GDP or apoforms, or Ser-tRNA^Sec and tRNA^Sec to SelB in any form, are similar ($K_d$ = 0.5 $\mu$M). Thermodynamic coupling in binding of Sec-tRNA^Sec and GTP to SelB ensures at the same time the specificity of Sec- versus Ser-tRNA^Sec selection and rapid release of Sec-tRNA^Sec from SelB after GTP cleavage on the ribosome. SelB provides an example for the evolution of a highly specialized protein-RNA complex toward recognition of unique set of identity elements. The mode of tRNA recognition by SelB is reminiscent of another specialized factor, eIF2, rather than of EF-Tu, the common delivery factor for all other aminoacyl-tRNAs, in line with a common evolutionary ancestry of SelB and eIF2.**

Selenocysteine (Sec),[2] the 21st genetically encoded amino acid, is typically located in the active sites of enzymes, most of which are involved in redox reactions. Incorporation of Sec into selenoproteins requires a specialized translation elongation factor SelB. SelB specifically recognizes selenocysteyl-tRNA, Sec-tRNA^Sec, but not other aminoacyl-tRNAs (aa-tRNAs) (1). In bacteria, tRNA^Sec is charged with serine by seryl-tRNA synthetase. The resulting Ser-tRNA^Sec is not recognized by the translation elongation factor EF-Tu and does not enter translation; rather, the seryl residue of Ser-tRNA^Sec is converted to a selenocysteyl residue by the pyridoxal phosphate-containing enzyme selenocysteine synthase (the *selA* gene product), which uses selenomonophosphate as the selenium donor substrate (2). The latter is synthesized from selenite and ATP by seleno-phosphate synthetase (the *selD* gene product). Finally, Sec-tRNA^Sec is recognized by SelB, which delivers it to ribosomes translating mRNAs coding for selenoproteins. The incorporation of Sec is encoded by a combination of an internal UGA stop codon and a specific mRNA hairpin structure, the SECIS (selenocysteine-inserting sequence) located immediately downstream of the UGA codon. In bacteria, SelB binds to the SECIS element directly, without the help of auxiliary proteins, thereby targeting Sec-tRNA^Sec to the specific UGA codon (3, 4).

SelB shares sequence similarity with other translation factors that carry aa-tRNAs to the ribosome, such as EF-Tu, which binds all elongator aa-tRNAs except for Sec-tRNA^Sec, eukaryotic eIF2$\gamma$, which is specific for the initiator Met-tRNA$_i$, or initiation factors IF2/eIF5B (5, 6). SelB consists of four domains that are arranged in a "chalice"-like fashion (7). SelB domains I (the GTP binding domain), II, and III have the same secondary structure elements as the respective domains of EF-Tu, provide most of the contact surface for Sec-tRNA^Sec, and are conserved among bacteria, archaea, and eukarya. The structure of domain IV of SelB, which has no analog in EF-Tu or other translational GTPases, is not conserved between pro- and eukaryotes (7–9). In bacterial SelB, winged helix motifs of domain IV recognize the hairpin backbone and nucleotides extruded from the SECIS helix (8).

The nucleotide-binding properties of SelB (10) differ markedly from those of EF-Tu (11) and rather resemble those of EF-G or IF2 (12, 13). SelB from *Escherichia coli* binds GTP and GDP with affinities of 0.7 $\mu$M and 13 $\mu$M, respectively (10). The rate of GDP dissociation from SelB is high, $15\ s^{-1}$, which allows for rapid and spontaneous nucleotide exchange, explaining the absence of a nucleotide exchange factor for SelB. In contrast to EF-Tu, which undergoes a large structural rearrangement when GTP is hydrolyzed to GDP, domains I-III in SelB from *Methanococcus maripaludis* adopt similar, GTP-like conformations in the presence of GTP, GDP, or in the absence of nucleotide (7), in line with the notion that SelB is able to bind Sec-tRNA^Sec not only in the GTP- but also the apo- and GDP-bound form (1, 7). This raises the questions of whether and how the GTP form of SelB is specifically recognized by Sec-tRNA^Sec. The structure of the SelB complex with Sec-tRNA^Sec is not available.

The current model of SelB action on the ribosome is largely based on the analogy to EF-Tu. The ternary complex EF-Tu·GTP·aa-tRNA binds to the ribosome and, upon recognition of a correct codon, hydrolyzes GTP. The following release of aa-tRNA from EF-Tu·GDP is rapid and spontaneous, because the affinity of aa-tRNA for EF-Tu·GDP is very low, and thus GTP hydrolysis by EF-Tu can be considered as an all-or-none switch for the release of aa-tRNA. Domains I-III of SelB are expected to bind to the ribosome in a similar fashion as the respective domains of EF-Tu; in that arrangement, domain IV

[2] The abbreviations used are: Sec, selenocysteine; EF-Tu, elongation factor Tu; DTT, dithiothreitol; aa-tRNA, aminoacyl-tRNA; GDPNP, guanosine 5′-$\beta\gamma$-imidodiphosphate.

of SelB reaches the mRNA entrance tunnel on the 30 S subunit (14, 15). GTP hydrolysis by SelB is required for selenocysteine incorporation into peptides (16). However, the role of GTP hydrolysis for SelB function is not clear, because, unlike EF-Tu, SelB binds its aa-tRNA also in the presence of GDP or in the absence of nucleotide (1, 7), albeit with unknown affinity.

In this work, we determined the effect of guanine nucleotides on the affinity of SelB for Sec-tRNA^Sec and developed a thermodynamic and kinetic framework for the formation of the ternary complex. We further estimated the relative contributions of the Sec residue and the tRNA^Sec molecule to the interaction with SelB, probed the nature of binding contacts, and determined the kinetics of Sec-tRNA^Sec release from SelB in either the GTP- or GDP-bound form.

## EXPERIMENTAL PROCEDURES

*Protein and tRNA Purification*—All proteins were expressed in BL21(DE3) cells. The plasmids coding for *E. coli* SelA and SelD were a gift from M. Wahl (Free University of Berlin). The plasmid coding for *E. coli* SelB (17) was a gift from A. Böck (LMU Munich). SelA was purified by ammonium sulfate precipitation as described (18) followed by gel filtration on Sephacryl S300 in buffer A (10 mM HEPES, pH 7.5, 3 mM DTT, 0.5 mM EDTA, 10 $\mu$M pyridoxal 5-phosphate). Histidine-tagged SelD, SerRS, and SelB were purified on Ni-nitrilotriacetic acid agarose (Qiagen) under non-denaturing conditions according to the manufacturer's protocol. SelD and SerRS were dialyzed against buffer B (50 mM HEPES, pH 7.5, 70 mM NH$_4$Cl, 30 mM KCl, 5 mM MgCl$_2$, 2 mM DTT). SelB was dialyzed against buffer C (50 mM HEPES, pH 7.5, 400 mM KCl, 5 mM MgCl$_2$, 2 mM DTT, 20% glycerol). All proteins were frozen in liquid nitrogen and stored at $-80$ °C. Concentrations of SelB were determined by absorbance at 280 nm ($\epsilon_{SelB} = 81080$ M$^{-1}$cm$^{-1}$). The preparation of SelB used for the experiments was free of GTP and GDP, as determined by HPLC analysis (19). The protein purity was better than 95% according to SDS-PAGE, and the activity in Sec-tRNA^Sec binding was >85% (16).

tRNA^Sec was overexpressed in *E. coli* BL21(DE3) transformed with the plasmid pCB2013 containing the *selC* gene under the control of its own promoter (18); the plasmid was a gift from A. Böck (LMU Munich). tRNA^Sec was purified as described (20). Fluorescence-labeled tRNA^Sec(Prf20) was prepared according to the protocol described for tRNA^Phe (21). Unmodified tRNA^Sec was prepared by T7-RNA polymerase transcription and purified under non-denaturating conditions on MonoQ 5/50 GL (GE Healthcare) (22). tRNA^Sec was aminoacylated and Ser-tRNA^Sec purified as described (16). To prepare Sec-tRNA^Sec, tRNA^Sec (10 $\mu$M), SerRS (6 $\mu$M), $^3$H- or $^{14}$C-labeled serine (30 $\mu$M), ATP (5 mM), inorganic pyrophosphatase (Sigma, 0.01 units/$\mu$l), SelA (3 $\mu$M), SelD (10 $\mu$M), Na$_2$SeO$_3$ (250 $\mu$M), SelB (6 $\mu$M), and GTP (2 mM) were incubated in buffer B with 7 mM MgCl$_2$. After incubation for 60 min at 37 °C, Sec-tRNA^Sec was phenol-extracted as described (16) and purified by gel filtration on Superdex 75 10/300 GL (GE Healthcare). The extent of conversion was >90%, as determined by thin layer chromatography (23) and the SelB binding assay (16). Native or transcribed tRNA^Sec were used in nitrocellulose filtration

assays where they showed identical affinities to SelB. Fluorescent tRNA^Sec (Prf) was prepared from native tRNA^Sec.

*Equilibrium Titrations*—All experiments were performed in buffer B at 25 °C unless stated otherwise. GDP was purified on a MonoQ (12) column. Constant amounts of Sec-tRNA^Sec were mixed with varying amounts of SelB in the absence or presence of GTP/GDP (2 mM) and incubated for 15 min. For reactions with very low amounts of protein (<1 pmol), 50 $\mu$g of bovine serum albumin (Fermentas) were added to the reactions to prevent unspecific adsorption of the protein to the tube walls. The amount of [$^{14}$C]Sec or [$^3$H]Sec bound to SelB was determined by filtration through nitrocellulose filters (0.45 $\mu$m, Sartorius). Filters were dissolved and radioactivity measured in Quickszint 361 scintillation mixture (Zinsser Analytic). The data were evaluated by non-linear fitting to a quadratic equation describing ligand binding to one site using Prism 5 (GraphPad Software, San Diego, CA). Equilibrium titrations with fluorescence-labeled tRNA^Sec(Prf20) were carried out in a PTI fluorimeter (excitation at 470 nm, emission at 510 nm). Increasing concentrations of SelB in the absence or presence of guanine nucleotide (2 mM) were added to a constant amount of tRNA^Sec(Prf20) or Ser-tRNA^Sec(Prf20) aminoacylated *in situ* (0.05 $\mu$M), and the increase of Prf fluorescence was monitored. The measured fluorescence was corrected for dilution and titrations were evaluated as described (24). $\Delta H°$ and $\Delta S°$ values were obtained from the slope and y-axis intercept of the $-\log(K_d)$ *versus* $1/T$ plot, respectively, at each ionic condition. The linear dependence of the $\Delta H°$ and $\Delta S°$ values on monovalent ions concentration allowed extrapolation to the ionic strength conditions used in other titration experiments, *i.e.* buffer B with 30 mM KCl.

The number of ion pairs formed between SelB and tRNA^Sec, Ser-tRNA^Sec, or Sec-tRNA^Sec was calculated from the slopes of $-\log(K_d)$ *versus* $-\log[M^+]$ plots according to Equation 1,

$$\log(K_d) = (Z\psi + k) \times \log[M^+] - \log(K^0) \qquad \text{(Eq. 1)}$$

where [M$^+$] is the total concentration of monovalent cations in the reaction (in moles); $\psi$ is the fraction of counterions associated with the nucleic acid per phosphate group; Z is the number of cations that interact with the nucleic acid; $k$ is the number of anions released from the protein upon formation of the ternary complex; $K^0$ is an intrinsic binding constant. The $\psi$ value takes into account the proportion of single-stranded and double-stranded regions of tRNA^Sec; an estimate was made on the basis of the crystal structures of EF-Tu·GDPNP·Phe-tRNA^Phe and EF-Tu·GDPNP·Cys-tRNA^Cys complexes (25, 26), which indicate that three-quarters of the groups that directly interact with EF-Tu were located in double-stranded regions of tRNA.

*Kinetic Measurements*—To determine the apparent association rate constants of complex formation, $k_{app}$, [$^3$H]Sec-tRNA^Sec (20 pM) was mixed with SelB (40 pM), GTP, or GDPNP (0.1 mM) in buffer B at 25, 30, and 37 °C. The amount of [$^3$H]Sec-tRNA^Sec bound to SelB was determined by nitrocellulose filtration. To measure dissociation rate constants, $k_{off}$, [$^3$H]Sec-tRNA^Sec (5 nM), SelB (7 nM), and GTP (or GDPNP) (2 mM) were incubated in buffer B for 15 min at the indicated temperature to form the complex, and then a 10-fold excess of unlabeled Sec-tRNA^Sec was added to follow the dissociation of

[³H]Sec-tRNA^Sec from the complex. The amount of Sec-tRNA^Sec was not changed significantly due to deacylation or oxidation during the time of experiment. Time courses were evaluated by single-exponential fitting using Prism software. The association rate constant, $k_{on}$, was calculated according to Equation 2,

$$k_{on} = (k_{app} - k_{off})/([SelB{\cdot}GTP] + [Sec\text{-}tRNA^{Sec}]) \quad \text{(Eq. 2)}$$

where [SelB·GTP] and [Sec-tRNA^Sec] denote equilibrium concentrations.

Rapid kinetics were measured with proflavin-labeled tRNA^Sec using a stopped-flow apparatus (SX-18MV; Applied Photophysics, Surrey, UK) in buffer B at 25 °C. Proflavin fluorescence was excited at 470 nm and measured after passing a longpass filter (KV 500; Schott, Mainz, Germany). SelB (0.4 μM, final concentrations after mixing are given throughout) was preincubated with the respective form of tRNA^Sec(Prf20) (0.2 μM), and the complexes were rapidly mixed with unlabeled tRNA^Sec (3 μM). Time courses depicted in the figures were obtained by averaging 8–10 individual transients. Data were evaluated by fitting to a single-exponential function with a characteristic time constant ($k_{app}$), amplitude ($A$), and another variable for the final signal ($F_\infty$) according to Equation 3,

$$F = F_\infty + A{\cdot}\exp(-k_{app} \times t) \quad \text{(Eq. 3)}$$

where $F$ is the fluorescence at time $t$. Where necessary, two exponential terms were used with two characteristic time constants ($k_{app1}$, $k_{app2}$), amplitudes ($A$, $B$), and another variable for the final signal ($F_\infty$) according to Equation 4.

$$F = F_\infty + A{\cdot}\exp(-k_{app1} \times t) + B{\cdot}\exp(-k_{app2} \times t)$$

$$\text{(Eq. 4)}$$

The reason for kinetic heterogeneity is not known; the average dissociation rate constant was estimated as described (29). Calculations were performed using Prism software. Standard deviations were calculated using the same software.

## RESULTS

*Affinity of SelB to tRNA*—We analyzed the complex formation between Sec-tRNA^Sec, Ser-tRNA^Sec, or tRNA^Sec and SelB in the apo-, GDP-, or GTP-bound forms, using nitrocellulose filtration or fluorescence titration techniques. In agreement with earlier observations (1, 7), Sec-tRNA^Sec binds to SelB in all three forms (Fig. 1A); however, the affinity of binding was found to be much higher for SelB·GTP than for the apo- or GDP-bound forms. With SelB·GTP the affinity was too high ($K_d < 1$ nM) to accurately determine the $K_d$ value under the reaction conditions used for these experiments. The affinity of Sec-tRNA^Sec for SelB-apo and SelB·GDP was similar with $K_d$ values of 420 nM and 540 nM, respectively (Table 1). The affinities for SelB of Sec-tRNA^Sec prepared from native tRNA or from a tRNA transcript were also similar, 420 and 470 nM, respectively (Fig. 1A, compare *open* and *closed squares*), indicating that unmodified tRNA^Sec behaves essentially the same as native tRNA^Sec with respect to SelB binding.
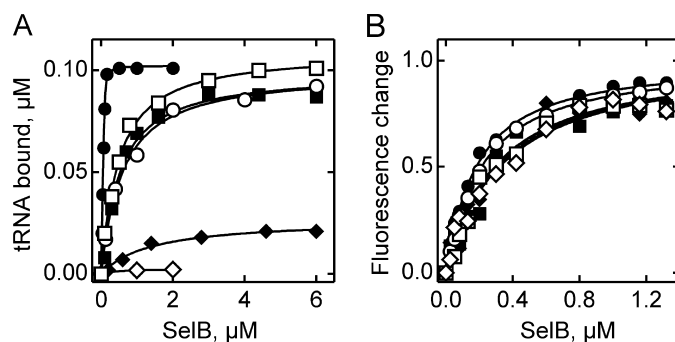


FIGURE 1. **Binding of SelB in the GTP-, GDP-, and apo-conformations to different forms of tRNA^Sec.** *A*, binding of native Sec-tRNA^Sec (0.1 μM) to SelB·GTP (●), SelB·GDP (○), SelB-apo (□), and Sec-tRNA^Sec prepared by T7-RNA polymerase transcription to SelB-apo (■) measured by nitrocellulose filtration. As controls, Phe-tRNA^Phe interaction with SelB·GTP (◆) and Sec-tRNA^Sec binding to a filter-immobilized SelB·GTP without incubation (◇) are shown. *B*, binding of Ser-tRNA^Sec(Prf20) to SelB·GTP (●), SelB·GDP (■), apo-SelB (◆), and of tRNA^Sec(Prf20) to SelB·GTP (○), SelB·GDP (□), and apo-SelB (◇) measured by equilibrium fluorescence titrations. The fluorescence changes (16–33%) were normalized by putting the maximum signal change to 1.

**TABLE 1**
**Summary of the $K_d$ values**

| | Nucleotide bound | | |
| | Apo | GDP | GTP |
|---|---|---|---|
| | *nM* | *nM* | *nM* |
| SelB·Sec-tRNA^Sec | 420 ± 30 | 540 ± 60 | $(2.1 \pm 0.6){\cdot}10^{-4}$ |
| SelB·Ser-tRNA^Sec | 270 ± 60 | 280 ± 60 | 160 ± 10 |
| SelB·tRNA^{Sec a} | 290 ± 50 | 280 ± 50 | 190 ± 10 |
| EF-Tu·Phe-tRNA^{Phe a} | N.D.^b | 28,500 | 0.85 |
| eIF2·Met-tRNA_i^{Met c} | 115 | 150 | 9 |
| eIF2·tRNA_i^{Met c} | N.D. | 140 | 130 |

^a The $K_d$ values were measured at 6 °C; data taken from Ref. 40.
^b N.D., not determined.
^c The $K_d$ values measured at 26 °C; data taken from Ref. 37.

The affinity of deacylated tRNA^Sec and Ser-tRNA^Sec to SelB was determined by fluorescence titrations using fluorescence-labeled tRNA^Sec(Prf20) containing proflavin at position 20 in the D loop (Fig. 1B). Using [¹⁴C]Ser-tRNA^Sec(Prf20), we verified that the two methods, nitrocellulose filtration and fluorescence titration, gave identical results and that fluorescence labeling did not impair function. The affinities of deacylated tRNA^Sec and Ser-tRNA^Sec for SelB, SelB·GDP, and SelB·GTP were very similar (Table 1).

*Kinetics of Sec-tRNA^Sec Binding to SelB*—As the affinity of Sec-tRNA^Sec binding to SelB·GTP was too high to be determined by titration at standard conditions, we set out to determine the kinetics of interaction and calculate the $K_d$ from $k_{on}$ and $k_{off}$ values. Time courses of Sec-tRNA^Sec binding to SelB·GTP (Fig. 2A) in excess of SelB·GTP over [³H]Sec-tRNA^Sec were single-exponential, and the concentration dependence of the apparent association constant, $k_{app}$, was linear (Fig. 2B), suggesting a well-behaved one-step binding reaction that followed pseudo-first order. As the ordinate intercept was close to zero (Fig. 2B), $k_{off}$ values were measured in separate chase experiments. The SelB·GTP·[³H]Sec-tRNA^Sec complex was formed, and the dissociation of [³H]Sec-tRNA^Sec was monitored after adding excess unlabeled Sec-tRNA^Sec (Fig. 2C). The resulting $k_{off}$ values, together with the $k_{on}$ values calculated from the $k_{app}$ and $k_{off}$ ("Experimental Procedures"), are summarized in Table 2. The $K_d$ values for the SelB·GTP·Sec-tRNA^Sec

complex, calculated from $K_d = k_{off}/k_{on}$, are in the subpicomolar range (Table 2), indicating an extremely tight association. For comparison, we also measured the association and dissociation rates and the $K_d$ value for the interaction of Sec-tRNA$^{Sec}$ with SelB in the complex with GDPNP, which is commonly used as a non-hydrolyzable GTP analog. Whereas the association rate constants of Sec-tRNA$^{Sec}$ with SelB·GTP or SelB·GDPNP were the same, the dissociation rates differed considerably, resulting in a 25-fold higher $K_d$ value of the complex with GDPNP. This suggests that the conformations of SelB with GTP and GDPNP are somewhat different. Therefore, the interactions between SelB and Sec-tRNA$^{Sec}$ that were modeled on the basis of the SelB·GDPNP crystal structure (7) may not reflect the GTP-containing complex in every detail.
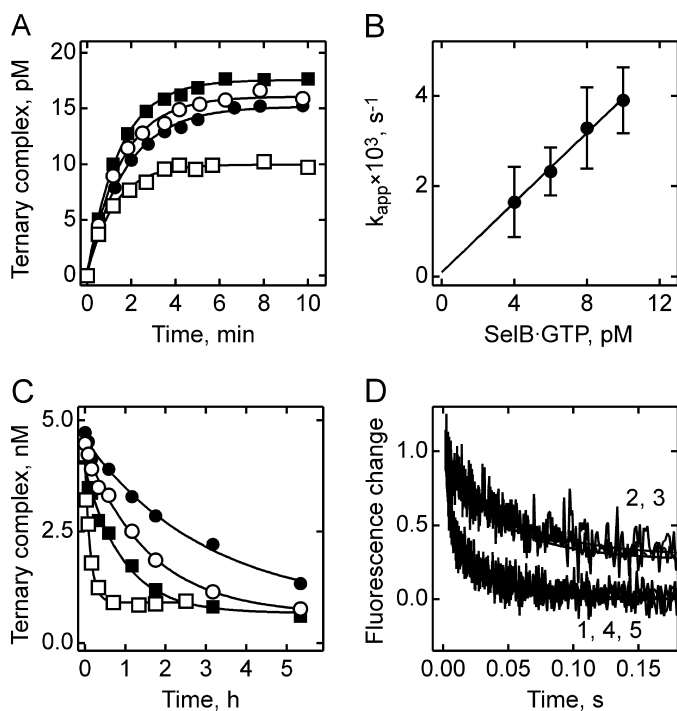


FIGURE 2. **Kinetics of tRNA$^{Sec}$-SelB interactions.** *A*, time courses of Sec-tRNA$^{Sec}$ binding to SelB·GTP at 25 °C (●), 30 °C (○), 37 °C (■), and to SelB·GDPNP at 37 °C (□). *B*, concentration dependence of the apparent rate constant of Sec-tRNA$^{Sec}$ binding to SelB·GTP at 25 °C. *C*, time courses of Sec-tRNA$^{Sec}$ dissociation from SelB·GTP·Sec-tRNA$^{Sec}$ at 25 °C (●), 30 °C (○), 37 °C (■), and from SelB·GDPNP·Sec-tRNA$^{Sec}$ at 37 °C (□); $k_{off}$ values are summarized in Table 2. *D*, time courses of dissociation of Sec-tRNA$^{Sec}$(Prf20) from the complex with SelB·GDP (1), Ser-tRNA$^{Sec}$(Prf20) from the complex with SelB·GTP (2), tRNA$^{Sec}$(Prf20) from SelB·GTP (3), SelB·GDP (4), and SelB-apo (5) at 25 °C. Traces in groups 1, 4, 5 and 2, 3 are indistinguishable.

The dissociation of Sec-tRNA$^{Sec}$ from the complex with SelB·GTP (or GDPNP) was very slow (in the hours range), allowing for the determination of $k_{off}$ by nitrocellulose filtration. In contrast, the dissociation of almost all other complexes was too rapid to be monitored by filtration. For those complexes, we measured dissociation rate constants by fluorescence stopped-flow (Fig. 2*D*). Complexes of SelB in the apo-, GDP-, or GTP-bound forms with Sec-, Ser-, and deacylated tRNA$^{Sec}$(Prf20) were mixed with excess unlabeled tRNA$^{Sec}$, and the release of the labeled tRNA$^{Sec}$ was monitored by the fluorescence decrease taking place in the milliseconds range. Using $k_{off}$ and $K_d$ values (Table 1), association rate constants $k_{on}$ were calculated (Table 2). Upon replacement of GTP for GDP, the dissociation of Sec-tRNA$^{Sec}$ from the complex became faster by more than six orders of magnitude, whereas the association rate was unchanged. The complexes of Ser-tRNA$^{Sec}$ and tRNA$^{Sec}$ with SelB·GTP also dissociated rapidly, five orders of magnitude faster than the SelB·GTP·Sec-tRNA$^{Sec}$ complex. The stability of the complexes of tRNA$^{Sec}$ with SelB was much less sensitive to the nucleotide form of the factor, with tRNA$^{Sec}$ dissociating from SelB·GTP only 10 times more slowly than from SelB·GDP or SelB.

*Effect of Ionic Strength on SelB·GTP·Sec-tRNA$^{Sec}$ Complex Formation*—To understand the molecular basis for the tight binding of Sec-tRNA$^{Sec}$ to SelB·GTP, we determined the ionic strength dependence of the $K_d$ values, which can provide information about the contribution of electrostatic interactions to complex formation (27). The experiments were carried out at 37 °C in the presence of increasing concentrations of KCl up to 525 mM (Fig. 3*A*). The decrease in affinity with increasing ionic strength of the buffer (Fig. 3*B*) suggests that ternary complex formation involves ionic interactions. The number of ion pairs contributing to the interaction was estimated from the slope of the plot (27, 28). The Mg$^{2+}$ concentration (4 mM free Mg$^{2+}$) was low compared with that of KCl; hence, the uncertainty in estimating the number of ionic interactions that is introduced by the presence of Mg$^{2+}$ ions was negligible. The number of ionic interactions involved in SelB·GTP·Sec-tRNA$^{Sec}$ formation was $4.2 \pm 0.2$. In comparison, the interaction of SelB with Ser-tRNA$^{Sec}$ or tRNA$^{Sec}$ was much less dependent on salt concentration (Fig. 3*B*), and the estimated number of ion pairs was 0.6. The different salt sensitivities of the SelB complex in the presence and absence of Sec argues against the possibility that the KCl effect is not due to electrostatics but to the effect of Cl$^-$ ions on the protein structure. Furthermore, the log($K_d$) value

**TABLE 2**

**Rate constants of formation and dissociation of various SelB complexes**

| | $k_{on}$ | $k_{off}$ | $K_d$ |
|---|---|---|---|
| | M$^{-1}$s$^{-1}$ | s$^{-1}$ | nM |
| SelB·GTP·Sec-tRNA$^{Sec}$ (25 °C) | $(4.2 \pm 0.3) \cdot 10^8$ | $(0.9 \pm 0.2) \cdot 10^{-4}$ | $(0.21 \pm 0.06) \cdot 10^{-3}$ [a] |
| SelB·GTP·Sec-tRNA$^{Sec}$ (30 °C) | $(4.9 \pm 0.3) \cdot 10^8$ | $(1.7 \pm 0.2) \cdot 10^{-4}$ | $(0.35 \pm 0.06) \cdot 10^{-3}$ [a] |
| SelB·GTP·Sec-tRNA$^{Sec}$ (37 °C) | $(5.1 \pm 0.2) \cdot 10^8$ | $(2.9 \pm 0.4) \cdot 10^{-4}$ | $(0.6 \pm 0.1) \cdot 10^{-3}$ [a] |
| SelB·GDPNP·Sec-tRNA$^{Sec}$ (37 °C) | $(3.8 \pm 2) \cdot 10^8$ | $(21 \pm 2) \cdot 10^{-4}$ | $(5.5 \pm 0.8) \cdot 10^{-3}$ [a] |
| SelB·GDP·Sec-tRNA$^{Sec}$ | $(4.4 \pm 1.2) \cdot 10^8$ [b] | $240 \pm 40$ | $540 \pm 60$ |
| SelB·GTP·Ser-tRNA$^{Sec}$ | $(0.9 \pm 0.2) \cdot 10^8$ [b] | $14 \pm 2$ | $160 \pm 10$ |
| SelB·GTP·tRNA$^{Sec}$ | $(1.0 \pm 0.1) \cdot 10^8$ [b] | $18 \pm 1$ | $190 \pm 10$ |
| SelB·GDP·tRNA$^{Sec}$ | $(8.0 \pm 2.7) \cdot 10^8$ [b] | $220 \pm 30$ | $280 \pm 50$ |
| SelB-apo·tRNA$^{Sec}$ | $(7.2 \pm 2.4) \cdot 10^8$ [b] | $210 \pm 30$ | $290 \pm 50$ |

[a] Calculated from the $k_{on}$ and $k_{off}$ values.
[b] Calculated using the $K_d$ values.

FIGURE 3. **Ionic strength dependence of tRNA$^{Sec}$, Ser-tRNA$^{Sec}$, and Sec-tRNA$^{Sec}$ binding to SelB·GTP.** *A*, binding of SelB·GTP to Sec-tRNA$^{Sec}$ in buffer B without NH$_4$Cl and with 150, 250, 350, 450, and 525 mM KCl (from *top* to *bottom*). *B*, dependence of $K_d$ values on monovalent ion concentration of SelB·GTP·Sec-tRNA$^{Sec}$ (●), SelB·GTP·Ser-tRNA$^{Sec}$(Prf20) (◆), and SelB·GTP·tRNA$^{Sec}$(Prf20) (◇). [M$^+$] is the total concentration of monovalent cations in the reaction (in moles).
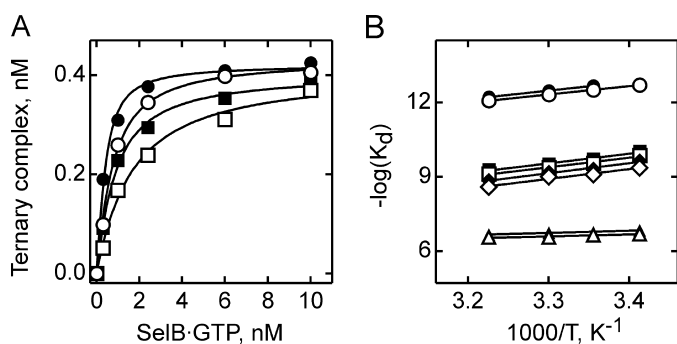


FIGURE 4. **Temperature dependence of tRNA$^{Sec}$, Ser-tRNA$^{Sec}$, and Sec-tRNA$^{Sec}$ binding to SelB·GTP.** *A*, binding of SelB·GTP to Sec-tRNA$^{Sec}$ in buffer B with 430 mM KCl at 20, 25, 30, and 37 °C (from *top* to *bottom*). *B*, temperature dependence of the $K_d$ values of SelB·GTP·tRNA$^{Sec}$(Prf20) (▲), SelB·GTP·Ser-tRNA$^{Sec}$(Prf20) (△), and SelB·GTP·Sec-tRNA$^{Sec}$ calculated from the rate constants of Sec-tRNA$^{Sec}$ binding to and dissociation from SelB·GTP (Fig. 2) (●), or extrapolated (○) from the temperature dependence of the $K_d$ values measured in buffer B with 480 mM KCl (◇), 430 mM KCl (◆), 380 mM KCl (□), and 330 mM KCl (■).

was a linear function of log[M$^+$] over the whole range of salt concentrations and similar slopes of the log($K_d$) *versus* log[M$^+$] plots were obtained for potassium chloride and acetate, suggesting that the contributions of unspecific anion effects are insignificant (27, 28).

*Thermodynamic Parameters of SelB·GTP·Sec-tRNA$^{Sec}$ Complex Formation*—We used two independent approaches to determine the thermodynamic parameters of SelB·GTP·Sec-tRNA$^{Sec}$ complex formation. The standard enthalpy and entropy changes were estimated using the $K_d$ values calculated from the rate constants (Fig. 4). Alternatively, we determined the thermodynamic parameters at several high KCl concentrations where affinities were reduced sufficiently to measure $K_d$ values reliably. The dependence of the $\Delta H°$ and $\Delta S°$ values on monovalent ions concentration was linear, which allowed for the extrapolation to other ionic strength conditions; both methods gave identical results (Table 3). The binding of Sec-tRNA$^{Sec}$ to SelB·GTP is driven by a large favorable enthalpy change, whereas the entropy change was very small. In comparison, with Ser-tRNA$^{Sec}$ and tRNA$^{Sec}$, the decrease in the affinity of binding to SelB·GTP was entirely due to a less favorable binding enthalpy, whereas the entropy changes were even slightly more favorable.

**TABLE 3**
Thermodynamic parameters of tRNA$^{Sec}$ binding to SelB·GTP

| | $\Delta H°$ | $\Delta G°$ | $T\Delta S°$ |
|---|---|---|---|
| | *kcal/mol, 25 °C* | *kcal/mol, 25 °C* | *kcal/mol, 25 °C* |
| Sec-tRNA$^{Sec}$ | $-16.0 \pm 0.6$ | $-17.3 \pm 0.2$ | $1.3 \pm 0.6$ |
| Ser-tRNA$^{Sec}$ | $-4 \pm 1$ | $-9.1 \pm 0.2$ | $5 \pm 1$ |
| tRNA$^{Sec}$ | $-4.0 \pm 0.8$ | $-9.2 \pm 0.2$ | $5.3 \pm 0.8$ |

## DISCUSSION

SelB, EF-Tu, eEF1A, and eIF2 are translation factors that deliver different aa-tRNAs to the ribosome. EF-Tu has evolved to bind all elongator aa-tRNAs, except for Sec-tRNA$^{Sec}$, with approximately the same affinity (30, 31). The thermodynamic contributions of the amino acid and the tRNA to the overall binding affinity are independent of and compensate for one another when the amino acid is cognate. In contrast, the affinities of EF-Tu for misacylated tRNAs may vary by several thousand-fold because of the lack of thermodynamic compensation (30, 32).

Unlike EF-Tu, SelB has evolved to bind a single aa-tRNA, Sec-tRNA$^{Sec}$, and the recognition pattern is specific for the SelB-Sec-tRNA$^{Sec}$ pair (Fig. 5). The tRNA$^{Sec}$ molecule is selected by SelB based on specific structural determinants, which distinguish tRNA$^{Sec}$ from all other tRNAs (33, 34). Upon binding of tRNA$^{Sec}$ or Ser-tRNA$^{Sec}$ to SelB, about one net ion pair is formed. Such contribution of ionic interactions is comparable to that in the EF-Tu·GTP·Phe-tRNA$^{Phe}$ complex (35). Importantly, the Ser residue is not recognized by SelB, as the affinity of the factor for Ser-tRNA$^{Sec}$ and deacylated tRNA$^{Sec}$ is similar and has almost identical binding enthalpy and entropy. The favorable entropy change upon binding is somewhat unexpected, given that complex formation should lead to a loss of degrees of freedom, but may reflect the contribution of nonionic interactions or release of ordered water molecules upon complex formation.

The affinity of Ser-tRNA$^{Sec}$ and tRNA$^{Sec}$ to SelB is independent of the guanine nucleotide. This suggests that the two tRNAs bind to SelB irrespective of the conformational changes in the G domain induced by nucleotide binding and is consistent with the similarity of the overall shape of the three SelB forms (7). In contrast, the Sec residue increases the binding affinity to SelB·GTP by six orders of magnitude, allowing for very efficient selection of Sec-tRNA$^{Sec}$ against binding of deacylated tRNA$^{Sec}$ or non-converted Ser-tRNA$^{Sec}$. That such discrimination may be crucial is demonstrated by the fact that the replacement of Sec by Ser in the active site of formate dehydrogenase H leads to the loss of the enzyme activity (36).

Another recognition element in the SelB system is the thermodynamic coupling between binding of Sec-tRNA$^{Sec}$ and GTP to SelB (Fig. 5). Whereas all three forms of tRNA$^{Sec}$ have similar affinities to SelB-apo or SelB·GDP, Sec-tRNA$^{Sec}$ appears to form additional interactions with SelB·GTP, resulting in a much more stable complex. The interaction may involve formation of salt bridges (see below) as well as other types of interactions (*e.g.* formation of additional hydrogen bonds), although their exact contribution to the strength of binding is unknown. The specific stabilization of the SelB·GTP·Sec-tRNA$^{Sec}$ complex ensures that Sec-tRNA$^{Sec}$ is

channeled to the active GTP-bound form of SelB, rather than to the GDP-bound or apoforms, which do not support translation (16). Furthermore, because the production of Sec-tRNA$^{Sec}$ consumes considerable cellular resources, Sec-tRNA$^{Sec}$ should be stringently protected by SelB from destruction by hydrolysis or oxidation. With respect to thermodynamic coupling, the ligand-binding properties of SelB are reminiscent of those of eIF2, which in the GTP-bound state forms an interaction with the methionine moiety of Met-tRNA$_i$ that is disrupted when GTP is replaced with GDP, while contacts between the factor and the body of the tRNA remain intact (37). These similarities in specific recognition and selection of one particular tRNA may indicate a common evolutionary ancestry of SelB and eIF2. In fact, phylogenetic studies suggest that SelB and eIF2 constitute an ancient subfamily of translation GTPases distinct from the EF-Tu/eEF1A subfamily (6).

Our data suggest that the recognition of the Sec residue of Sec-tRNA$^{Sec}$ results in the net formation of about three ion pairs. These pairs might involve the Sec group directly or reflect the formation upon Sec binding of salt bridges between other groups, *e.g.* of additional interactions with the phosphate groups of tRNA$^{Sec}$ or salt bridges within SelB. The important contribution of these ionic interactions is consistent with the large favorable change in binding enthalpy of SelB·GTP binding to Sec-tRNA$^{Sec}$ compared with tRNA$^{Sec}$ or Ser-tRNA$^{Sec}$. Modeling of the aminoacyl-binding pocket of SelB suggested a potential role for residues Asp-180, Arg-181, and Arg-236 (5). Asp-180 and Arg-236 are conserved among SelB orthologs from all kingdoms, whereas Arg-181 is present in bacterial proteins and is replaced by His in archaeal and eukaryal SelB (His-192 in *M. maripaludis* (7)). Residues Arg-181 and Arg-236 provide positive charges that could interact with the negatively charged selenolate group formed by deprotonation of the selenol group of Sec-tRNA$^{Sec}$ (p$K_a$ of the group in free selenocysteine is 5.2) (38). The importance of these residues for Sec binding was corroborated by mutational analysis, which suggested that the presence of at least one positive charge in the aminoacyl-binding pocket of SelB is required for function (7). The identity of other group(s) contributing to ionic interactions is currently unknown.

Another role for thermodynamic coupling may be to ensure that Sec-tRNA$^{Sec}$ is released rapidly from SelB after GTP hydrolysis on the ribosome. Upon binding of the SelB·GTP·Sec-tRNA$^{Sec}$ to the ribosome in a codon- and SECIS-directed manner, GTP hydrolysis occurs and Sec-tRNA$^{Sec}$ is released from SelB·GDP to accommodate in the ribosomal A site. For most elongator aa-tRNAs, the accommodation step is rate-limiting for peptide bond synthesis (39). If Sec-tRNA$^{Sec}$ were to bind SelB·GDP too tightly, the release of Sec-tRNA$^{Sec}$ from the factor and its accommodation on the ribosome would be slow, and, as a consequence, peptide bond formation would also be slow. GTP hydrolysis by SelB increases the rate of Sec-tRNA$^{Sec}$ release by six orders of magnitude, from $10^{-4}$ s$^{-1}$ to 240 s$^{-1}$; the latter rate appears sufficiently high to allow for rapid transfer of Sec-tRNA$^{Sec}$ from the factor to the ribosome. In this view, thermodynamic coupling in binding of Sec-tRNA$^{Sec}$ and GTP to SelB ensures both the specificity of Sec- *versus* Ser-tRNA$^{Sec}$
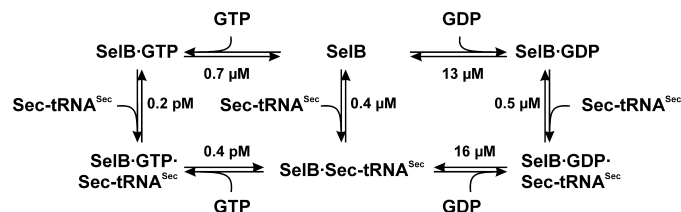


FIGURE 5. **A thermodynamic framework of the interactions between Sec-tRNA^Sec, SelB, and guanine nucleotides.** $K_d$ values of the respective interactions are indicated. The values for Sec-tRNA$^{Sec}$ binding are from this report; for GTP/GDP binding to SelB are from Ref. 10; and for GTP/GDP binding to SelB·Sec-tRNA$^{Sec}$ are calculated from the law of mass action.

selection and the efficient protection of Sec-tRNA$^{Sec}$ against premature degradation, combined with the rapid release of Sec-tRNA$^{Sec}$ on the ribosome after GTP hydrolysis.

## REFERENCES

1. Forchhammer, K., Leinfelder, W., and Böck, A. (1989) *Nature* **342,** 453– 456
2. Commans, S., and Böck, A. (1999) *FEMS Microbiol. Rev.* **23,** 335–351
3. Atkins, J. F., and Gesteland, R. F. (2000) Nature **407,** 463– 465
4. Baron, C., and Böck, A. (1995) in *tRNA: Structure Biosynthesis, and Function* (Soll, D., and RajBhandary, U., eds), pp. 529 –544, American Society for Microbiology, Washington
5. Hilgenfeld, R., Böck, A., and Wilting, R. (1996) *Biochimie* **78,** 971–978
6. Keeling, P. J., Fast, N. M., and McFadden, G. I. (1998) *J. Mol. Evol.* **47,** 649 – 655
7. Leibundgut, M., Frick, C., Thanbichler, M., Böck, A., and Ban, N. (2005) *EMBO J.* **24,** 11–22
8. Yoshizawa, S., Rasubala, L., Ose, T., Kohda, D., Fourmy, D., and Maenaka, K. (2005) *Nat. Struct. Mol. Biol.* **12,** 198 –203
9. Selmer, M., and Su, X. D. (2002) *EMBO J.* **21,** 4145– 4153
10. Thanbichler, M., Bock, A., and Goody, R. S. (2000) *J. Biol. Chem.* **275,** 20458 –20466
11. Gromadski, K. B., Wieden, H. J., and Rodnina, M. V. (2002) *Biochemistry* **41,** 162–169
12. Wilden, B., Savelsbergh, A., Rodnina, M. V., and Wintermeyer, W. (2006) *Proc. Natl. Acad. Sci. U.S.A.* **103,** 13670 –13675
13. Milon, P., Tischenko, E., Tomsic, J., Caserta, E., Folkers, G., La Teana, A., Rodnina, M. V., Pon, C. L., Boelens, R., and Gualerzi, C. O. (2006) *Proc. Natl. Acad. Sci. U.S.A.* **103,** 13962–13967
14. Hüttenhofer, A., and Böck, A. (1998) in *RNA Structure and Function*, pp. 603– 639, Cold Spring Harbor Laboratory Press, NY
15. Ose, T., Soler, N., Rasubala, L., Kuroki, K., Kohda, D., Fourmy, D., Yoshizawa, S., and Maenaka, K. (2007) *Structure* **15,** 577–586
16. Fischer, N., Paleskava, A., Gromadski, K. B., Konevega, A. L., Wahl, M. C., Stark, H., and Rodnina, M. V. (2007) *Biol. Chem.* **388,** 1061–1067
17. Thanbichler, M., and Böck, A. (2003) *Protein. Expr. Purif.* **31,** 265–270
18. Thanbichler, M., and Böck, A. (2002) *Methods Enzymol.* **347,** 3–16
19. John, J., Sohmen, R., Feuerstein, J., Linke, R., Wittinghofer, A., and Goody, R. S. (1990) *Biochemistry* **29,** 6058 – 6065
20. Kothe, U., Paleskava, A., Konevega, A. L., and Rodnina, M. V. (2006) *Anal. Biochem.* **356,** 148 –150
21. Wintermeyer, W., and Zachau, H. G. (1974) *Methods Enzymol.* **29,** 667– 673
22. Konevega, A. L., Soboleva, N. G., Makhno, V. I., Semenkov, Y. P., Wintermeyer, W., Rodnina, M. V., and Katunin, V. I. (2004) *RNA* **10,** 90 –101
23. Leinfelder, W., Forchhammer, K., Veprek, B., Zehelein, E., and Böck, A.

(1990) *Proc. Natl. Acad. Sci. U.S.A.* **87,** 543–547

24. Rodnina, M. V., Pape, T., Fricke, R., Kuhn, L., and Wintermeyer, W. (1996) *J. Biol. Chem.* **271,** 646–652

25. Nissen, P., Kjeldgaard, M., Thirup, S., Polekhina, G., Reshetnikova, L., Clark, B. F., and Nyborg, J. (1995) *Science* **270,** 1464–1472

26. Nissen, P., Thirup, S., Kjeldgaard, M., and Nyborg, J. (1999) *Structure* **7,** 143–156

27. Record, M. T., Jr., Lohman, M. L., and De Haseth, P. (1976) *J. Mol. Biol.* **107,** 145–158

28. Lohman, T. M., deHaseth, P. L., and Record, M. T., Jr. (1980) *Biochemistry* **19,** 3522–3530

29. Milon, P., Konevega, A. L., Gualerzi, C. O., and Rodnina, M. V. (2008) *Mol. Cell* **30,** 712–720

30. LaRiviere, F. J., Wolfson, A. D., and Uhlenbeck, O. C. (2001) *Science* **294,** 165–168

31. Louie, A., and Jurnak, F. (1985) *Biochemistry* **24,** 6433–6439

32. Asahara, H., and Uhlenbeck, O. C. (2002) *Proc. Natl. Acad. Sci. U.S.A.* **99,** 3499–3504

33. Baron, C., and Böck, A. (1991) *J. Biol. Chem.* **266,** 20375–20379

34. Rudinger, J., Hillenbrandt, R., Sprinzl, M., and Giegé, R. (1996) *EMBO J.* **15,** 650–657

35. Abrahamson, J. K., Laue, T. M., Miller, D. L., and Johnson, A. E. (1985) *Biochemistry* **24,** 692–700

36. Axley, M. J., Böck, A., and Stadtman, T. C. (1991) *Proc. Natl. Acad. Sci. U.S.A.* **88,** 8450–8454

37. Kapp, L. D., and Lorsch, J. R. (2004) *J. Mol. Biol.* **335,** 923–936

38. Huber, R. E., and Criddle, R. S. (1967) *Arch. Biochem. Biophys.* **122,** 164–173

39. Pape, T., Wintermeyer, W., and Rodnina, M. V. (1998) *EMBO J.* **17,** 7490–7497

40. Dell, V. A., Miller, D. L., and Johnson, A. E. (1990) *Biochemistry* **29,** 1757–1763